

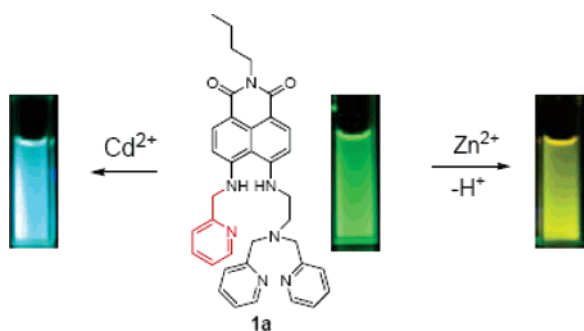
**Ratiometric and Highly Selective Fluorescent Sensor for Cadmium under Physiological pH Range: A New Strategy to Discriminate Cadmium from Zinc**

Chunliang Lu,<sup>†</sup> Zhaochao Xu,<sup>†</sup> Jingnan Cui,<sup>\*,†</sup> Rong Zhang,<sup>†</sup> and Xuhong Qian<sup>\*,‡</sup>

State Key Laboratory of Fine Chemicals, DUT – KTH Joint Education and Research Center on Molecular Devices, Dalian University of Technology, Dalian 116012, China, and Shanghai Key Laboratory of Chemical Biology, East China University of Science and Technology, Shanghai 200237, China

jncui@dlut.edu.cn; xhqian@ecust.edu.cn

Received January 7, 2007



In a neutral aqueous environment, a new ratiometric  $\text{Cd}^{2+}$  fluorescent sensor **1a** can successfully discriminate  $\text{Cd}^{2+}$  from  $\text{Zn}^{2+}$  by undergoing two different internal charge transfer (ICT) processes, and the high selectivity of sensor **1a** to  $\text{Cd}^{2+}$  over some other metals was also observed. Moreover, through structure derivation and a series of NMR studies, the unique role of the 2-picolyl group (the part in red in the abstract graphic) in the sensor **1a**– $\text{Cd}^{2+}$  complexation was disclosed.

Cadmium, whose half-life in humans is estimated to be between 15 and 20 years,<sup>1</sup> is listed by the U.S. Environmental Protection Agency as one of 126 priority pollutants. Excessive exposure to cadmium will lead to pulmonary cancer and probably cause some nonpulmonary cancers, such as prostatic and renal cancers.<sup>2</sup> The use of fluorescent  $\text{Cd}^{2+}$  sensors could help to reveal the cadmium carcinogen mechanism in vivo as well as to monitor cadmium concentration temporally in the environment.

So far, only few fluorescent cadmium sensors have been reported,<sup>3</sup> and there are many aspects left to be improved, such as unsuitable pH range for physiological use and lack of sensitivity. More importantly, it is still a challenge to develop

fluorescent sensors that can discriminate  $\text{Cd}^{2+}$  from  $\text{Zn}^{2+}$ . Because cadmium and zinc are in the same group of the Periodic Table and have similar properties, they usually cause similar spectral changes after interactions with fluorescent sensors (including the change of intensity and the shift of wavelengths). In other words, the existence of one of the cation pair will provide false positive signals mimicking the presence of the other cation.

Two major approaches have proved helpful in solving this discrimination problem for the development of  $\text{Cd}^{2+}$  fluorescent sensors. One approach is based on the formation of an anthracene– $\text{Cd}(\text{II})$   $\pi$ -complex.<sup>3b,d,g</sup> Though it results in the red-shifted emission, its performance suffers from the low affinity of the anthracene– $\text{Cd}(\text{II})$  complex, and hence, its sensitivity is expected to improve. The other one, involving exciton-coupled circular dichroism signals to assist fluorescence, has achieved the differentiation of the multiple analytes,<sup>4</sup> but its expensive and inconvenient nature block it from practical use. Herein, we developed a new strategy for discrimination of cadmium and zinc based on the simple internal charge transfer (ICT) mechanism.

The ICT mechanism has been widely exploited for cation sensing.<sup>5</sup> If the electron-donating character of the electron-donating group is reduced, blue shifts of both the absorption and fluorescence spectra are expected. Conversely, if a cation promotes the electron-donating character of the electron-donating group, the absorption and fluorescence spectra should be red-shifted. In previous research, we have successfully designed and synthesized two ratiometric fluorescent sensors for  $\text{Cu}^{2+}$  based on the above two different ICT processes separately.<sup>6</sup> Therefore, it is reasonable to predict that, if the receptor moiety is properly designed, only one sensor molecule could realize two above-mentioned reverse ICT processes to sense two different analytes. In addition, our recently reported  $\text{Zn}^{2+}$  ratiometric fluorescent sensor,<sup>7</sup> which was based on the deprotonation mechanism of the same system, inspired us for further exploration.

Bearing this conception in mind, we designed and synthesized a series of fluorescent sensors **1** (Figure 1) for  $\text{Cd}^{2+}$  and  $\text{Zn}^{2+}$  based on the 4,5-diamino-1,8-naphthalimide as the fluorophore. Di-2-picolylamine (DPA) was introduced as part of the receptor, which has a higher affinity to  $\text{Zn}^{2+}$  than group I and group II cations<sup>8</sup> but usually shows similar selectivity and affinity to  $\text{Cd}^{2+}$ . To distinguish between  $\text{Zn}^{2+}$  and  $\text{Cd}^{2+}$ , another pyridine

(3) (a) Bronson, R. T.; Michaelis, D. J.; Lamb, R. D.; Hussein, G. A.; Farnsworth, P. B.; Linford, M. R.; Izatt, R. M.; Bradshaw, J. S.; Savage, P. B. *Org. Lett.* **2005**, *7*, 1105. (b) Gunnlaugsson, T.; Lee, T. C.; Parke, R. *Org. Lett.* **2003**, *5*, 4065. (c) Costero, A. M.; Andreu, R.; Monrabal, E.; Martinez-Manez, R.; Sancenon, F.; Soto, J. J. *Chem. Soc., Dalton Trans.* **2002**, 1769. (d) Choi, M.; Kim, M.; Lee, K. D.; Han, K. N.; Yoon, I. A.; Chung, H. J.; Yoon, J. *Org. Lett.* **2001**, *3*, 3455. (e) Prodi, L.; Bolletta, F.; Montalti, M.; Zaccaroni, N. *Eur. J. Inorg. Chem.* **1999**, *3*, 455. (f) Lu, J. Z.; Zhang, Z. *J. Analyst* **1995**, *120*, 453. (g) Huston, M. E.; Engleman, C.; Czarnik, A. W. *J. Am. Chem. Soc.* **1990**, *112*, 7054. (h) Akkaya, E. U.; Huston, M. E.; Czarnik, A. W. *J. Am. Chem. Soc.* **1990**, *112*, 3590.

(4) Castagnetto, J. M.; Canary, J. W. *Chem. Commun.* **1998**, 203.  
 (5) (a) Valeur, B.; Leray, I. *Coord. Chem. Rev.* **2000**, *205*, 3. (b) de Silva, A. P.; Gunaratne, H. Q. N.; Gunnlaugsson, T.; Huxley, A. J. M.; McCoy, C. P.; Rademacher, J. T.; Rice, T. E. *Chem. Rev.* **1997**, *97*, 1515.  
 (6) (a) Xu, Z.; Qian, X.; Cui, J. *Org. Lett.* **2005**, *7*, 3029. (b) Xu, Z.; Xiao, Y.; Qian, X.; Cui, J.; Cui, D. *Org. Lett.* **2005**, *7*, 889.  
 (7) Xu, Z.; Qian, X.; Cui, J.; Zhang, R. *Tetrahedron* **2006**, *62*, 10117.

<sup>†</sup> Dalian University of Technology.

<sup>‡</sup> East China University of Science and Technology.

(1) Jin, T.; Lu, J.; Nordberg, M. *Neurotoxicology* **1998**, *19*, 529.

(2) (a) Waalkes, M. P. *Mutat. Res.* **2003**, *533*, 107. (b) Waisberg, M.; Joseph, P.; Hale, B.; Beyersmann, D. *Toxicology* **2003**, *192*, 95.

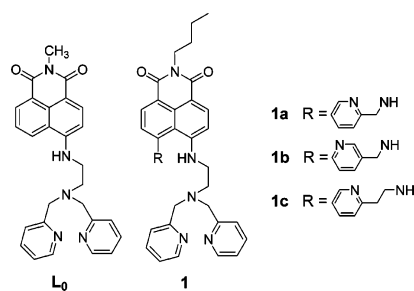
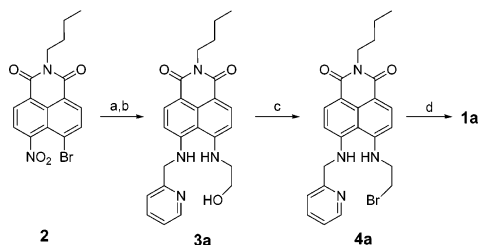


FIGURE 1. Molecular structures **L**<sub>0</sub>, **1a**, **1b**, and **1c**.

SCHEME 1. Synthesis of **1a**<sup>a</sup>



<sup>a</sup> Reagents and conditions: (a)  $\text{CH}_3\text{OCH}_2\text{CH}_2\text{OH}$ , 2-(aminomethyl)pyridine, heated; (b)  $\text{CH}_3\text{CN}$ , 2-aminoethanol, reflux; (c)  $\text{CH}_2\text{Cl}_2$ ,  $\text{PBr}_3$ , rt; (d)  $\text{CH}_3\text{CN}$ , DPA, KI,  $\text{K}_2\text{CO}_3$ , reflux.

moiety was involved as the supplemental group. The result showed that sensor **1a**, whose receptor was composed of the 2-picolyl group and DPA, successfully underwent the reverse ICT processes in sensing  $\text{Cd}^{2+}$  and  $\text{Zn}^{2+}$ . This sensing process not only results in ratiometric measurement, which can reduce the influence of the environments (such as temperature, polarity, and probe concentration), but also causes two different shifts of wavelength, which is more conspicuous and convenient for discrimination.

As shown in Scheme 1, the synthesis of sensor **1a** was started from compound **2**, which was prepared according to the published procedure.<sup>6b</sup> In the first step, compound **3a** was obtained by a two-step substitution reaction of compound **2** with 2-(aminomethyl)pyridine and 2-aminoethanol. Then, compound **4a** was synthesized via bromination reaction in the presence of  $\text{PBr}_3$ , which further reacted with DPA to yield **1a**.

The influence of pH on the fluorescence of **1a** was first determined by fluorescence titration in ethanol–water (1:9, v/v) solutions (Supporting Information, Figure S1). The fluorescence of free **1a** at 531 nm remained unaffected between pH 10.0 and 6.8 and then gradually decreased from pH 6.6 to 1.8 with a  $\text{pK}_a$  value of 4.0 due to a photoinduced electron transfer (PET) from the fluorophore to the protonated 2-picolyl group.<sup>6b,7</sup> Therefore, further fluorescence studies were carried out at pH 7.2 maintained with HEPES buffer (50 mM).

Figure 2 displays the absorption spectra of sensor **1a** taken in the course of titration with  $\text{Cd}^{2+}$  and  $\text{Zn}^{2+}$ . The absorption spectrum of free **1a** exhibited a maximum centered at 460 nm. When 1.0 equiv of  $\text{Cd}^{2+}$  was added, the absorption maxima did not shift, whereas the intensity of the maxima exhibited a little decrease with an isosbestic point at 420 nm (Figure 2a).

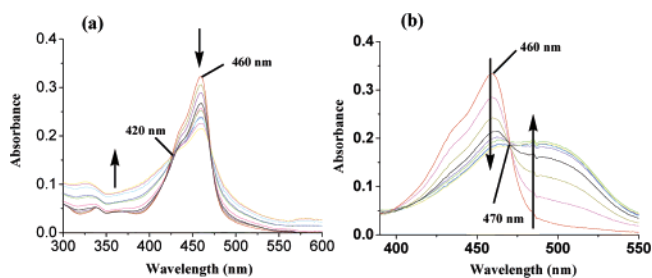


FIGURE 2. (a) Changes in the absorption spectra of **1a** ( $10 \mu\text{M}$ ) upon titration of  $\text{Cd}^{2+}$ ,  $[\text{Cd}^{2+}] = 0\text{--}10 \mu\text{M}$ ; (b) Changes in the absorption spectra of **1a** ( $10 \mu\text{M}$ ) upon titration of  $\text{Zn}^{2+}$ ,  $[\text{Zn}^{2+}] = 0\text{--}10 \mu\text{M}$ . All data were obtained in ethanol–water solutions (1:9, v/v, 50 mM HEPES buffer, pH = 7.2).

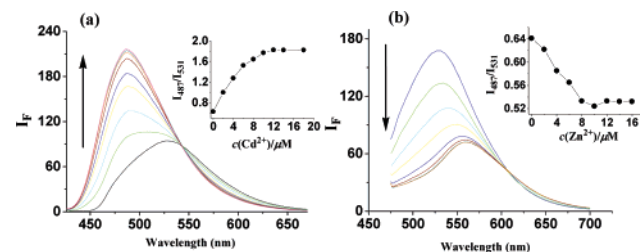


FIGURE 3. (a) Changes in the fluorescence emission spectra of **1a** ( $10 \mu\text{M}$ ) upon titration of  $\text{Cd}^{2+}$  ( $\lambda_{\text{ex}} = 420 \text{ nm}$ ). Inset: Ratiometric calibration curve  $I_{487}/I_{531}$  as a function of  $\text{Cd}^{2+}$  concentration. (b) Changes in the fluorescence emission spectra of **1a** ( $10 \mu\text{M}$ ) upon titration of  $\text{Zn}^{2+}$  ( $\lambda_{\text{ex}} = 470 \text{ nm}$ ). Inset: Ratiometric calibration curve  $I_{487}/I_{531}$  as a function of  $\text{Zn}^{2+}$  concentration. All data were obtained in ethanol–water solutions (1:9, v/v, 50 mM HEPES buffer, pH = 7.2).

On the other hand, upon the addition of 1 equiv of  $\text{Zn}^{2+}$ , the intensity of the absorption maxima at 460 nm dropped prominently and simultaneously a red-shifted absorption peak centered at 492 nm was developed, illustrating that  $\text{Zn}^{2+}$  coordination led to the increase of the electron-donating ability of the fluorophore's nitrogen moiety (Figure 2b).

When excitation was at the isosbestic point of 420 nm, the emission maxima of **1a** blue-shifted from 531 to 487 nm with the sequential addition of  $\text{Cd}^{2+}$  (Figure 3a). Such a prominent blue shift suggested the reduction of the electron-donating ability of the NH moiety upon the coordination with  $\text{Cd}^{2+}$ , and a clear isoemission point at 542 nm indicated the coexistence of the free sensor **1a** and the **1a** +  $\text{Cd}^{2+}$  complex. The interaction of **1a** with  $\text{Zn}^{2+}$  also showed ratiometric fluorescent signals. The emission maxima were red-shifted 27 nm from 531 to 558 nm with an isoemission point at 610 nm, and the fluorescence color changed from blue to yellow. The insets of fluorescence titration spectra (Figure 3) demonstrated that **1a** can form a 1:1 adduct with  $\text{Cd}^{2+}$  or  $\text{Zn}^{2+}$ . When the **1a** +  $\text{Cd}^{2+}$  complex was formed, the  $\Phi_{\text{F}}$  value increased from 0.27 to 0.60, and it decreased to 0.23 with saturated  $\text{Zn}^{2+}$ .<sup>9</sup> The associate constant  $K_s$  (**1a** +  $\text{Zn}^{2+}$ ), derived from the titration curve, was  $1.65 \times 10^5 \text{ M}^{-1}$ . On the other hand, the inserted titration curve with  $\text{Cd}^{2+}$  was too steep to be used for the determination of a reliable constant. So, a further titration experiment was carried out with a more dilute solution ( $2 \mu\text{M}$ ) (Supporting Information, Figure S2), and the associate constant  $K_s$  (**1a** +  $\text{Cd}^{2+}$ ) was determined to be

(8) (a) Lim, N. C.; Brückner, C. *Chem. Commun.* **2004**, 1094. (b) Fan, J.; Wu, Y.; Peng, X. *Chem. Lett.* **2004**, 33, 1392. (c) Burdette, S. C.; Frederickson, C. J.; Bu, W.; Lippard, S. J. *J. Am. Chem. Soc.* **2003**, 125, 1778. (d) Maruyama, S.; Kikuchi, K.; Hirano, T.; Urano, Y.; Nagano, T. *J. Am. Chem. Soc.* **2002**, 124, 10650. (e) Kim, T. W.; Park, J.; Hong, J. *J. Chem. Soc., Perkin Trans. 2* **2002**, 923.

(9) The quantum yield ( $\Phi_{\text{F}}$ ) was determined by using *N*-butyl-4-butylamino-1,8-naphthalimide in absolute ethanol ( $\Phi_{\text{F}} = 0.81$ ) as a standard. Alexiou, M. S.; Tychoopoulos, V.; Ghorbanian, S.; Tyman, J. H. P.; Brown, R. G.; Brittain, P. I. *J. Chem. Soc., Perkin Trans. 2* **1990**, 837.

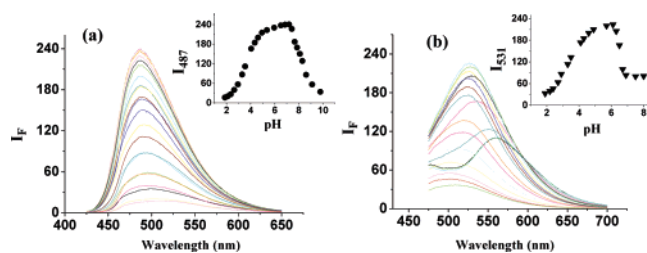


**FIGURE 4.** (a) Influence of pH on the fluorescence of the **1a** + Cd<sup>2+</sup> adduct (1:1<sup>1a</sup> = [Cd<sup>2+</sup>] = 10 μM) in ethanol–water solutions (1:9, v/v) (λ<sub>ex</sub> = 420 nm). Inset: Changes in the relative intensity at 487 nm as a function of pH. (b) Influence of pH on the fluorescence of the **1a** + Zn<sup>2+</sup> adduct (1:1<sup>1a</sup> = [Zn<sup>2+</sup>] = 10 μM) in ethanol–water solutions (1:9, v/v) (λ<sub>ex</sub> = 470 nm). Inset: Changes in the relative intensity at 531 nm as a function of pH. pH value was adjusted by HClO<sub>4</sub> and tetramethylammonium hydroxide.

$5.75 \times 10^5 \text{ M}^{-1}$ . Furthermore, it can be predicted that Cd<sup>2+</sup> could be detected at least down to  $1.0 \times 10^{-7} \text{ M}$  when **1a** was employed at 2 μM in 50 mM HEPES buffer aqueous solution.

Consistent with our previous research, sensor **1a** chelated Zn<sup>2+</sup> through a deprotonation process of the NH moiety of the naphthalimide,<sup>7</sup> which was reflected by the pH titration profile of sensor **1a** in the presence of Zn<sup>2+</sup> (Figure 4b). When the pH value decreased from 6.9 to 6.1, a gradual blue shift of the emission maxima was observed, much like the reverse process of sequential addition of Zn<sup>2+</sup>. At pH 6.1, the emission maximum centered at 558 nm, which stood for the **1a** + Zn<sup>2+</sup> adduct, vanished, and the free **1a** emission peak at 531 nm as well as the quantum yield (Φ<sub>F</sub> returned to 0.27) were recovered, suggesting the entire dissociation of the **1a** + Zn<sup>2+</sup> adduct at a low pH value. A pK<sub>a2</sub> value (**1a** + Zn<sup>2+</sup>) of 6.5 was derived from the process. On the contrary, the decrease of the pH value from 10.0 to 2.0 did not result in significant wavelength shifts to the **1a** + Cd<sup>2+</sup> adduct (Figure 4a). Derived from the fluorescence enhancement process from pH 10.0 to 7.0, the pK<sub>a2</sub> value of the **1a** + Cd<sup>2+</sup> adduct was determined to be 8.2, implying the protonation of the tertiary amine of DPA.<sup>10</sup> Even though the fluorescence of **1a** + Cd<sup>2+</sup> was influenced by pH, its intensity at 487 nm and the ratio of fluorescence intensity (*I*<sub>487</sub>/*I*<sub>531</sub>) were almost constant at the pH range from 5.0 to 7.8 (Supporting Information, Figure S3), indicating sensor **1a**'s potential for physiological use.

The deprotonation process induced by Zn<sup>2+</sup> was then confirmed by HRMS using ESI as the ion source (Figure 5). Peak *m/z* 600.1649 and 622.1346 values corresponded to [**1a** + H]<sup>+</sup> and [**1a** + Na]<sup>+</sup>, respectively (Figure 5a). When 1.0 equiv of Zn<sup>2+</sup> was added, the peaks of [**1a** + H]<sup>+</sup> and [**1a** + Na]<sup>+</sup> disappeared and the new peak at 662.0725 corresponding to [**1a** + Zn – H]<sup>+</sup> (the calculated value was 662.2222) was formed (Figure 5b), indicating that the deprotonation process did proceed in the ground state.

The fluorescence titration of **1a** with various metal ions was conducted to examine its selectivity (Supporting Information, Figure S4). Inheriting the merit of DPA appended sensors, sensor **1a** was exempt from the influence of a high concentration

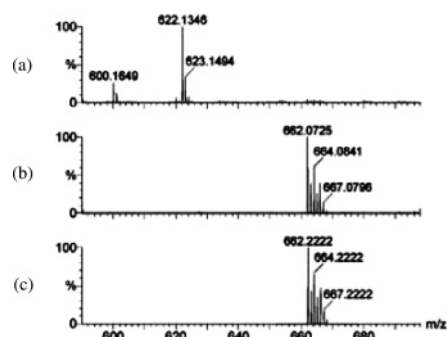


**FIGURE 5.** (a) HRMS spectrum of free **1a** (10 μM) in ethanol. (b) HRMS spectrum of the **1a** + Zn<sup>2+</sup> complex (10 μM) in ethanol. (c) Calculated pattern of the **1a** + Zn<sup>2+</sup> complex.<sup>11</sup>

of the physiologically abundant cations, including Na<sup>+</sup>, K<sup>+</sup>, Ca<sup>2+</sup>, and Mg<sup>2+</sup>. Furthermore, it was also silent to Pb<sup>2+</sup> and Fe<sup>3+</sup> and particularly exhibited high selectivity to Cd<sup>2+</sup> over Zn<sup>2+</sup>. Even though the addition of Zn<sup>2+</sup> decreased the intensity of the emission maxima to some extent, the ratio of fluorescence intensity at 487 nm to that at 531 nm was little disturbed, from 1.86 (without Zn<sup>2+</sup>) to 1.67 (with Zn<sup>2+</sup>) (Supporting Information, Figure S5). Some other metals, such as Hg<sup>2+</sup>, Ni<sup>2+</sup>, and Ag<sup>+</sup>, quenched the fluorescence to some extent, but the intensity of the emission maxima and the ratio of fluorescence intensity (*I*<sub>487</sub>/*I*<sub>531</sub>) were enhanced upon addition of an equivalent of Cd<sup>2+</sup>. Unfortunately, when the heavy quenchers Co<sup>2+</sup> and Cu<sup>2+</sup> existed, the enhancement was not observed.

Di-2-picolyamine (DPA) has been extensively used in Zn<sup>2+</sup>-selective sensors for its high affinity and excellent selectivity.<sup>12</sup> However, it is still difficult for fluorescent sensors with DPA as receptors to differentiate between Cd<sup>2+</sup> and Zn<sup>2+</sup>. Previously reported sensor **L0**,<sup>8b</sup> with a structure similar to sensor **1a**, only showed fluorescence enhancement both for Zn<sup>2+</sup> and Cd<sup>2+</sup> with nominal wavelength shifts. To have deeper insight into the selectivity–structure relationships of sensor **1a**, derivatives **1b** and **1c** (Figure 1) were synthesized and the following NMR studies were carried out for the underlying reasons.

As shown in Figure 6, the pyridine group of DPA and the 2-picoyl group played different roles in coordination. Upon the interaction with Zn<sup>2+</sup> or Cd<sup>2+</sup>, the protons 1 and 1', the ortho-positioned protons of DPA, experienced the proximately 0.3 ppm downfield shift to 8.6. These identical shifts were caused by the deshielding effect of the metal ion through the direct N-metal interactions,<sup>14</sup> which demonstrated the same role of DPA upon Cd<sup>2+</sup>/Zn<sup>2+</sup> chelation. On the other hand, when **1a**

(11) The data presented here were the original ones without the mass calibration. Commonly, the acceptable accuracy range of the HRMS spectra to characterize the compound structure should be under 10 mmu (millimass units). However, under the test concentration (10 μM), the signal was comparatively weak and easily disturbed by the environment, which caused it to be hard to calibrate, and consequently, the acceptable error increased to as high as 200 mmu. In addition, the HRMS test was also tried under a fluorescence spectra test situation—ethanol–water solutions (1:9, v/v, 50 mM HEPES buffer, pH = 7.2) and [**1a**] = [Zn<sup>2+</sup>] = 10 μM—but it failed to get satisfactory results due to the great impact of the high concentration of HEPES. The data were measured on Q-ToF Micro (Micromass Inc., Manchester, England), using ESI as the ion source. In addition, HRMS did not detect the existence of [**1a** + Cd<sup>2+</sup> – H]<sup>+</sup> species.

(12) Jiang, P.; Guo, Z. *Coord. Chem. Rev.* **2004**, *248*, 205.

(13) The peaks were assigned to the protons according to the H–H COSY spectra (see Supporting Information).

(14) The Zn<sup>2+</sup> coordination that promoted the deshielding effect of DPA was observed in the recent paper: McDonough, M. J.; Reynolds, A. J.; Lee, W. Y. G.; Jolliffe, K. A. *Chem. Commun.* **2006**, 2971.

(10) See selected references for the influence of pH on the fluorescence of DPA-containing sensors: (a) Lim, N. C.; Schuster, J. V.; Porto, M. C.; Tanudra, M. A.; Yao, L.; Freake, H. C.; Brückner, C. *Inorg. Chem.* **2005**, *44*, 2018. (b) Nolan, E. M.; Lippard, S. J. *Inorg. Chem.* **2004**, *43*, 8310. (c) Burdette, S. C.; Walkup, G. K.; Spingler, B.; Tsien, R. Y.; Lippard, S. J. *J. Am. Chem. Soc.* **2001**, *123*, 7831.

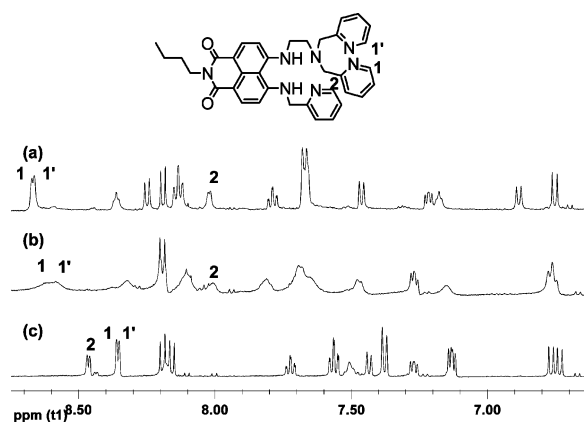
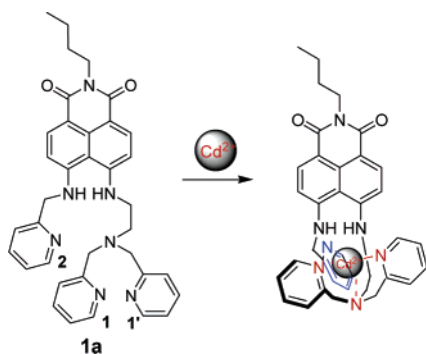


**FIGURE 6.** Partial  $^1\text{H}$  NMR spectra (500 MHz) of **1a** (10 mM) in DMSO (top): (a) **1a** + 1.0 equiv of  $\text{Zn}^{2+}$ ; (b) **1a** + 1.0 equiv of  $\text{Cd}^{2+}$ ; (c) free **1a**.<sup>13</sup>

**SCHEME 2. Proposed Binding Mechanisms for 1a with  $\text{Cd}^{2+}$  in the Ground State**



interacted with  $\text{Zn}^{2+}$  or  $\text{Cd}^{2+}$ , the proton 2, which was in the ortho position of the nitrogen atom of the 2-picoyl group, experienced a clear 0.34 ppm upfield shift from 8.46 to 8.12 (Figure 6). It possibly resulted from pyridine–metal  $\pi$ -d orbital interactions indicating the indirect pyridine–metal interactions through space. Meanwhile, both the absorption and fluorescence spectra of sensors **1b** and **1c** showed almost no changes (including the intensity and wavelength) toward  $\text{Zn}^{2+}$  or  $\text{Cd}^{2+}$  (Supporting Information, Figures S6 and S7). Consistent with their photophysical performance, the upfield shifts of the proton 2 of sensors **1b** and **1c** were much smaller, suggesting their invalid interactions with  $\text{Cd}^{2+}$  or  $\text{Zn}^{2+}$ .

Therefore, the supplemental pyridine group played an important part in the sensing process. As shown in Scheme 2, a cavity was constructed for sensing  $\text{Cd}^{2+}$  by DPA and the supplemental pyridine moiety. Although the main function of DPA was to grasp the metal cation through direct N–metal interactions, the additional pyridine moiety contributed more to the construction of the cavity in space promising the right size and suitable conformation. The 2-picoyl moiety (sensor **1a**) was demonstrated to be the most suitable one for the cavity, and any change to this moiety, including twist (sensor **1b**), flexibility (sensor **1c**), or omission (sensor **L<sub>0</sub>**), would lead to ineffective interactions of the analytes with the fluorophore in the excited state, subsequently resulting in failure to discriminate  $\text{Cd}^{2+}$  from  $\text{Zn}^{2+}$ .

In summary, on the basis of undergoing two reverse ICT processes in sensing  $\text{Cd}^{2+}$  and  $\text{Zn}^{2+}$ , sensor **1a** has demonstrated a new strategy to discriminate between this cation pair in a more

conspicuous and convenient way. Good selectivity to  $\text{Cd}^{2+}$  over some other cations, including  $\text{Zn}^{2+}$ , was also achieved. Moreover, the comparison of the photophysical properties and NMR signals between the derivatives (**1b** and **1c**) and sensor **1a** revealed the unique role of the 2-picoyl group in the sensing process. The design strategy of the sensor will help to improve the development of fluorescent sensors for discriminating other ion pairs, and the special structure–selectivity relationships may give some insight into how to construct receptors with special properties.

**Experimental Section**

**4a.** To an ice cold solution of **3a** (250 mg, 0.60 mmol) in dichloromethane (20 mL) was added dropwise ca. 5 mL of  $\text{PBr}_3$ . After that, the reaction mixture was further stirred at room temperature for an additional period of 3 h. The reaction was quenched with ice-cold water, and the pH was adjusted to 7–8. The organic portion was extracted with dichloromethane, and the solvent was removed under a vacuum. The crude product was chromatographed on silica gel (100–200 mesh). Elution of the column with a mixture of methanol and dichloromethane (1:20) gave 124 mg (43%) of **4a**. Mp: 183.7~184.9 °C.  $^1\text{H}$  NMR (DMSO, 400 MHz)  $\delta$  0.91 (t,  $J = 7.2$  Hz, 3H), 1.30 (m,  $J = 7.2$  Hz, 2H), 1.56 (m,  $J = 7.2$  Hz, 2H), 3.74 (t,  $J = 6.0$  Hz, 2H), 3.83 (t,  $J = 6.0$  Hz, 2H), 3.98 (t,  $J = 7.2$ , 2H), 4.69 (s, 2H), 6.79 (d,  $J = 8.8$  Hz, 1H), 6.96 (d,  $J = 8.8$  Hz, 1H), 7.36 (t,  $J = 7.6$  Hz, 1H), 7.40 (d,  $J = 8.4$  Hz, 1H), 7.53 (d,  $J = 8.0$  Hz, 1H), 7.84 (t,  $J = 8.0$  Hz, 1H), 8.18 (d,  $J = 8.4$  Hz, 1H), 8.19 (s, N–H), 8.25 (d,  $J = 8.8$  Hz, 1H), 8.61 (d,  $J = 4.4$  Hz, 1H).  $^{13}\text{C}$  NMR (DMSO, 100 MHz)  $\delta$  13.66, 19.73, 29.79, 31.66, 38.58, 45.53, 48.23, 122.13, 122.69, 131.74, 132.95, 133.12, 137.51, 148.37, 151.84, 151.91, 156.47, 163.16, 163.21. IR (KBr,  $\text{cm}^{-1}$ ) 3336, 2955, 2931, 2871, 1675, 1632, 1594, 1433, 1406, 1360, 810, 751. MS (APCI)  $[\text{M} + \text{H}]^+$  481.

**1a.** To a solution of **4a** (50 mg, 0.10 mmol) in acetonitrile were added 2 equiv of KI (35 mg), 2 equiv of  $\text{K}_2\text{CO}_3$  (29 mg), and 2 equiv of DPA (37  $\mu\text{L}$ ). After the reaction mixture had been moderately heated and refluxed for over 6 h, all the volatile components were evaporated and the residue was partitioned between dichloromethane and water. The organic phase was washed with water (3  $\times$  50 mL), then dried in  $\text{Na}_2\text{SO}_4$ . Flash chromatographic purification (dichloromethane–methanol = 20:1) afforded **1a** (46 mg, 74% yield). Mp: 122.6~124.4 °C.  $^1\text{H}$  NMR ( $\text{CD}_3\text{OD}$ , 400 MHz)  $\delta$  0.97 (t,  $J = 7.6$  Hz, 3H), 1.40 (m,  $J = 7.6$  Hz, 2H), 1.64 (m,  $J = 7.6$  Hz, 2H), 3.04 (t,  $J = 6.0$  Hz, 2H), 3.37 (t,  $J = 6.0$  Hz, 2H), 3.80 (s, 4H), 4.06 (t,  $J = 7.2$ , 2H), 4.63 (s, 2H), 6.58 (d,  $J = 8.5$  Hz, 2H), 6.73 (d,  $J = 8.5$  Hz, 2H), 7.04 (t,  $J = 6$  Hz, 2H), 7.27 (t,  $J = 6$  Hz, 1H), 7.35 (d,  $J = 7.6$  Hz, 2H), 7.45 (t,  $J = 8.0$  Hz, 3H), 7.73 (t,  $J = 7.6$  Hz, 1H), 8.13 (d,  $J = 8.5$  Hz, 1H), 8.24 (t,  $J = 4.5$  Hz, 3H), 8.51 (d,  $J = 4.8$  Hz, 2H).  $^{13}\text{C}$  NMR (DMSO, 100 MHz)  $\delta$  13.81, 19.87, 29.94, 41.39, 48.35, 52.03, 59.47, 106.28, 106.49, 109.50, 109.62, 110.08, 121.72, 122.07, 122.46, 122.84, 131.84, 133.13, 136.88, 137.58, 148.72, 152.12, 152.85, 156.65, 158.74, 163.33. IR (KBr,  $\text{cm}^{-1}$ ) 3322, 2954, 2924, 2853, 2816, 1673, 1631, 1587, 1405, 1355, 1310, 1145, 1089, 995, 968, 832, 811, 750. MS (APCI)  $[\text{M} + \text{H}]^+$  600. HRMS (ES+), calcd for  $\text{C}_{36}\text{H}_{37}\text{N}_7\text{O}_2$   $[\text{M} + \text{H}]^+$  600.3087, found 600.3080.

**Acknowledgment.** We are grateful to the National Key Project for Basic Research (2003CB114400) and the National Natural Science Foundation of China for financial support of this research. We also thank Dr. Yunkou Wu for valuable suggestions and discussions.

**Supporting Information Available:** Synthesis and characterization of compounds **1a–3a**, NMR, and spectroscopic data. This material is available free of charge via the Internet at <http://pubs.acs.org>.

JO070033Y